Molecular Biology of the Cell
Vol. 20, 581–588, January 15, 2009

Sterols Are Mainly in the Cytoplasmic Leaflet of the Plasma Membrane and the Endocytic Recycling Compartment in CHO Cells

Mousumi Mondal, Bruno Mesmin, Sushmita Mukherjee, and Frederick R. Maxfield

Department of Biochemistry, Weill Cornell Medical College, New York, NY 10065

Submitted July 31, 2008; Revised October 21, 2008; Accepted November 6, 2008
Monitoring Editor: Sandra L. Schmid

The transbilayer distribution of many lipids in the plasma membrane and in endocytic compartments is asymmetric, and this has important consequences for signaling and membrane physical properties. The transbilayer distribution of cholesterol in these membranes is not properly established. Using the fluorescent sterols, dehydroergosterol and cholestatrienol, and a variety of fluorescence quenchers, we studied the transbilayer distribution of sterols in the plasma membrane (PM) and the endocytic recycling compartment (ERC) of a CHO cell line. A membrane impermeant quencher, 2,4,6-trinitrobenzene sulfonic acid, or lipid-based quenchers that are restricted to the exofacial leaflet of the plasma membrane only reduce the fluorescence intensity of these sterols in the plasma membrane by 15–32%. When the same quenchers have access to both leaflets, they quench 70–80% of the sterol fluorescence. Sterol fluorescence in the ERC is also quenched efficiently in the permeabilized cells. In microinjection experiments, delivery of quenchers into the cytosol efficiently quenched the fluorescent sterols associated with the PM and with the ERC. Quantitative analysis indicates that 60–70% of the PM sterol is in the cytoplasmic leaflet. This means that cholesterol constitutes ~40 mol% of cytoplasmic leaflet lipids, which may have important implications for intracellular cholesterol transport and membrane domain formation.

INTRODUCTION

Biological membranes often have a pronounced asymmetry in the transbilayer distribution of lipids, and this can have important functional consequences. In mammalian cell plasma membranes (PM), the cytoplasmic leaflets are enriched in phosphatidylethanolamine (PE) and phosphatidylserine (PS), whereas the exofacial leaflets is enriched in sphingomyelin (SM; Pomorski and Menon, 2006; van Meer *et al.*, 2008). The negative electrical charge on the cytoplasmic leaflet of the PM, which is mainly created by PS and phosphoinositides, permits strong electrostatic interactions with peripheral cationic proteins (Yeung *et al.*, 2008). The elevated concentration of SM in the outer leaflet of the PM, combined with a high level of cholesterol, would promote formation of a liquid-ordered (l_o) phase.

Although cholesterol is one of the most abundant lipid molecules in the PM and plays important regulatory roles in biological processes, there is great uncertainty about its transbilayer distribution. The reported values for the amount of cholesterol in the outer leaflet ranges from as little as 13% in a study of mouse synaptic membranes (Hayashi *et al.*, 2002), to as much as 67% in human erythrocytes (Fisher, 1976). A major reason for these disparities has been the lack of suitable techniques to study transbilayer sterol distribution in living cells. In one of the earliest reports on this subject, cholesterol was reported to be enriched in the outer leaflet of human erythrocytes based on freeze-fracture studies (Fisher, 1976). Though elegant, some steps in this analysis could potentially perturb the transbilayer distribution of cholesterol. For example, cells were stored in acid citrate dextrose solution at 0–5°C to bind to the substrate. Also perplexing is the finding that the inner/outer leaflet ratio of cholesterol more than doubled when the buffer system was changed from phosphate-buffered saline to Tris-buffered saline.

Because the flip-flop rate of cholesterol in biological membranes at 37°C is high, with a $t_{1/2}$ of about a second or less (Steck *et al.*, 2002), methods that analyze binding of filipin (Blau and Bittman, 1978) or reaction with cholesterol oxidase (Gottlieb, 1977; Brasaemle *et al.*, 1988) are difficult to interpret because the sterol could flip many times during the assay, but even a transient appearance in the outer leaflet could be recorded in these assays as outer leaflet sterol.

Fluorescence quenching by molecules such as 2,4,6-trinitrobenzene sulfonic acid (TNBS), heavy atoms, or spin-labels is immediately reversed after the molecules separate, so quenching can provide an ongoing instantaneous measure of the proximity of the fluorophores and the quenchers. A polar-quenching molecule such as TNBS can only quench lipid fluorophores in the leaflet to which it has access, so it can be used to measure the transbilayer distribution of flu-

This article was published online ahead of print in *MBC in Press* (http://www.molbiolcell.org/cgi/doi/10.1091/mbc.E08–07–0785) on November 19, 2008.

Address correspondence to: Frederick R. Maxfield (frmaxfie@med.cornell.edu).

Abbreviations used: CHO, Chinese hamster ovary; CTL, cholestatrienol; DHE, dehydroergosterol; ERC, endocytic recycling compartment; MβCD, methyl-β-cyclodextrin; PC, phosphatidylcholine; PE, phosphatidylethanolamine; PM, plasma membrane; SLO, streptolysin-O; SLPC, spin-labeled phosphatidylcholine; SM, sphingomyelin; TNBS, 2,4,6-trinitrobenzene sulphonic acid.

orescent lipids. TNBS has been used in fluorometric studies of cells in suspension to quench the fluorescence of dehydroergosterol (DHE) and cholestatrienol (CTL), fluorescent sterols that serve as good cholesterol mimetics in both biochemical and cell biological studies (Hao *et al.*, 2002; Bjorkqvist *et al.*, 2005). Both of these probes have membrane orientation and dynamics similar to cholesterol (Scheidt *et al.*, 2003). CTL is nearly as effective as cholesterol in its condensing effect on 1-palmitoyl-2-oleoyl-sn-glycero-3-phosphocholine (POPC) membranes, and DHE is somewhat less effective (Hyslop *et al.*, 1990). Both of these sterol analogs have been used as reporter molecules associated with detergent-resistant membranes or ordered domains in model membranes (Wang *et al.*, 2004) and in cells (Hao *et al.*, 2001). Moreover, PM sterol distribution in cell surface structures has been studied using DHE (Wustner, 2007).

In studies of erythrocytes, TNBS was incubated with the cells at pH 8.5 for 45 min at 4°C to allow covalent cross-linking of the TNBS to glycoproteins and glycolipids on the PM, and it was found that only a small fraction of DHE in human erythrocyte membranes was quenched by the attached TNBS (Schroeder *et al.*, 1991), whereas the majority of DHE was quenched in rat and mice erythrocytes (Hale and Schroeder, 1982). The effects of these preincubations on the sterol distribution are not known. In a study in platelets (Boesze-Battaglia *et al.*, 1996) TNBS was added to suspensions of CTL-labeled cells, and it was reported that 65% of CTL fluorescence was quenched. In our hands, TNBS causes significant absorption of the excitation light used for CTL fluorescence in a cuvette, requiring a large "inner filter" correction; but this correction was not discussed in this report.

Previous studies of transbilayer distribution of cholesterol for nucleated cells were carried out using isolated PM preparations from a fibroblast cell line (Hale and Schroeder, 1982) and from synaptic PMs (Hayashi *et al.*, 2002). It is likely that the purification could perturb the transbilayer distribution of cholesterol.

We have developed fluorescence imaging techniques to observe the subcellular distribution of DHE and CTL (Hao *et al.*, 2002). This has several important advantages for studies of the distribution of sterols in living cells and for the study of the transbilayer distribution of sterols. Because we are observing the sterol fluorescence, we can directly evaluate the incorporation and distribution of the sterols in cells. This avoids problems associated with fluorescent sterols that are not associated with cells or labeling of dead cells. By delivering quenchers to the cytoplasm, we can evaluate the transbilayer sterol distribution in organelles such as the endocytic recycling compartment (ERC), which contains ~35–40% of the sterol in Chinese hamster ovary (CHO) cells (Hao *et al.*, 2002). Because the path length of illumination is very short, there is negligible absorption of light by TNBS, and this allows us to use instantaneous quenching methods, which avoid lengthy labeling procedures.

We examined the susceptibility of DHE and CTL in CHO cells to quenching by TNBS and by slowly flipping lipid-based quenchers. Herein we report that sterols are mainly distributed in the cytoplasmic leaflet of the PM and the ERC.

MATERIALS AND METHODS

Materials

DHE, cholesterol, TNBS, methyl-β-cyclodextrin (MβCD), biotin *N*-hydroxysuccinimide ester (biotin NHS ester), human transferrin (Tf), and streptavidin were from Sigma Chemical Co. (St. Louis, MO). CTL and 1-palmitoyl-2-(4-doxyl)-pentanoyl-*sn*-glycero-3-phosphocholine (4-SLPC) were synthesized by Dr. J. David Warren (Weill Cornell Medical College) following published protocols (Fischer *et al.*, 1984; Fellmann *et al.*, 1994). 1-Palmitoyl-2-stearoyl (11–12 dibromo)-*sn*-glycero-3-phosphocholine (11–12-Br_2PC), 12-SLPC, 1-palmitoyl-2-stearoyl (6–7 dibromo)-*sn*-glycero-3-phosphocholine (6–7-Br_2PC), 5-SLPC, 1-palmitoyl-2-oleoyl-*sn*-glycero-3-phosphocholine (POPC), 1-palmitoyl-2-oleoyl-*sn*-glycero-3-phosphoethanolamine (POPE), 1-palmitoyl-2-oleoyl-*sn*-glycero-3-[phospho-L-serine] (sodium salt; POPS), egg SM, and 1,2-distearoyl-*sn*-glycero-3-phosphoethanolamine-*N*-(biotinyl) (N-biotinyl PE) were from Avanti Polar lipids (Alabaster, AL), and *N*-[6(7-nitro-2-1,3-benzoxidiazol-4-yl)amino]dodecanoyl]-sphingosine-1-phosphocholine(C_6-NBD-SM), C_{12}-NBD SM, and Alexa-633 labeling kit were purchased from Invitrogen (Rockville, MD). Succinimidyl ester of Alexa-633 was conjugated to the iron-loaded Tf following the manufacturer's instructions. Solvents were of spectrophotometric grade from Sigma-Aldrich (Milwaukee, WI). Streptolysin-O (SLO) was obtained from Murex Diagnostics (Atlanta, GA). Cell culture supplies were from Invitrogen.

Cell Culture

TRVb1, a modified CHO cell line expressing the human Tf receptor, was grown as described previously (McGraw *et al.*, 1987). Cells for microscopy were plated 2 d before the experiment in 35-mm plastic tissue culture dishes with a 7-mm hole at the bottom covered by poly-D-lysine–coated coverslips (Salzman and Maxfield, 1989). Microscopy experiments on round cells were done after plating the cells for 16–20 h. Medium 1 (150 mM NaCl, 5 mM KCl, 1 mM $CaCl_2$, 1 mM $MgCl_2$, and 20 mM HEPES, pH 7.4) supplemented with 2 g/l glucose was used for incubations and during microscopy.

M19 cells, mutant CHO cells that are partial auxotrophs for cholesterol due to a deficiency of the gene S2P (Xu *et al.*, 2005), were a gift from Dr. T. Y. Chang (Dartmouth, NH). M19 cells were grown in medium containing lipoprotein-depleted serum and supplemented with 10 μg/ml DHE as described in detail in Supplementary Methods. Cholesterol and DHE content in the cells were measured by gas chromatography (Supplementary Methods). After 7 d, ~50% of cellular sterol was DHE.

Incorporation of Lipid Analogs into Cell Membranes

Lipid analog fluorescence quenchers were loaded onto fatty acid free bovine serum albumin (BSA) and then incubated with cells as described (Mukherjee *et al.*, 1999; 0.6 mM quencher in 20 mg/ml BSA). For labeling with NBD-SM analogs, cells were washed with ice-cold medium 1/glucose, chilled briefly on ice, incubated with 10 μM C_6-NBD-SM or C_{12}-NBD-SM on fatty-acid free BSA for 10 min on ice, washed extensively with medium 1/glucose, and imaged immediately. Cells were labeled with DHE/CTL-MβCD complexes (0.5 mM) as described (Hao *et al.*, 2002).

Delivery of TNBS to the Cytosol

Membrane Permeabilization by Mechanical Perforation. TRVb1 cells were labeled with DHE-MβCD and were permeabilized using a nitrocellulose membrane overlay and removal as described (Simons and Virta, 1987). Cells were transferred to high-potassium buffer (10 mM HEPES, 140 mM KCl, pH 7.4) containing propidium iodide (1 μg/ml) to identify the permeabilized cells.

SLO Permeabilization. DHE-labeled cells were perforated using the pore-forming bacterial toxin, SLO, as described (Martys *et al.*, 1995). After SLO treatment at 0°C, cells were transferred to high-potassium buffer containing 1 μg/ml propidium iodide and warmed for 6 min at 37°C.

Microinjection. TNBS (100 mM in pipette) was microinjected into DHE-labeled cells using back-loaded glass capillaries and a micromanipulator (Narishige, Greenvale, NY). Approximately 5–10% of the cell volume was introduced by injection. Rhodamine dextran (Rh-dextran; 0.25 mg/ml) was coinjected to identify the injected cells.

Liposome Preparation

Large unilamellar vesicles (LUVs) were made by extrusion technique (Mayer *et al.*, 1986). Briefly, 0.5 nmol of total lipids were mixed uniformly in chloroform/methanol (2:1) and dried under a stream of argon. Remaining traces of solvent were removed by placing them under vacuum for 1 h. Multilamellar vesicles were produced by dispersing dry lipids in phosphate-buffered saline (10 mM NaH_2PO_4, 140 mM NaCl, pH 7.4) with vortex mixing. LUVs were made by freeze-thawing multilamellar vesicles five times and then extruded 21 times through polycarbonate filters of pore size (400 nm).

Fluorescence Microscopy

Fluorescence microscopy and digital image acquisition were carried out using a Leica DMIRB microscope (Leica, Germany) optimized for DHE/CTL imaging, as described (Mukherjee *et al.*, 1998; Hao *et al.*, 2002; Wustner *et al.*, 2002). A Princeton Instruments (Princeton, NJ) cooled CCD camera was driven by MetaMorph Imaging System software (Universal Imaging, Downingtown, PA). All images were acquired using a 63×, 1.4 NA oil immersion objective.

C_6-NBD-SM and C_{12}-NBD-SM were imaged using a fluorescein filter cube, propidium iodide and Rh-dextran were imaged using a rhodamine filter cube, and Alexa-633 Tf was imaged using Cy 5 filter cube.

Quantification of DHE/CTL in the PM and the ERC

Images were first background-corrected using off-cell intensity values. Boxes (1.5 × 1.5 μm) were drawn in peripheral regions of the cells that lacked observable organelles to measure the PM-associated fluorescence (Supplementary Figure S2). Care was taken not to use regions adjacent to the nucleus, which would have the highest level of intracellular organelles. In our experimental conditions autofluorescence in these peripheral regions was negligible (<10%) compared with the fluorescence of cells labeled with DHE or CTL. To measure the DHE/CTL fluorescence in the ERC, boxes were drawn in the center of the perinuclear bright region identified previously as the ERC (Hao *et al.*, 2002). For round cells, PM-associated fluorescence were measured by drawing tiny boxes (0.75 × 0.75 μm) in the ring-like PM regions. Measurements were made in the identical regions within 30 s after addition of quencher, and data from at least 30 cells were acquired for each condition. Typically, measurements were made from 15 to 20 boxes on the PM and four boxes on the ERC in each cell. Intensity measurements were corrected for photobleaching as described (Mukherjee *et al.*, 1998). For photobleaching correction, images were excited with light for the same time period as with the quencher, but in this case without addition of any quencher. Photobleaching correction was done on each experimental day and averaged over several fields. The average photobleaching correction factor was ~10%.

RESULTS

Quenching of DHE Fluorescence by TNBS in Liposomes

To validate the use of TNBS as a quencher of DHE in the exofacial leaflet, we made LUVs with lipid compositions that mimic those in the outer leaflet and inner leaflet of the PM (Schroeder *et al.*, 1998; Dietrich *et al.*, 2001; Wang and Silvius, 2001). The liposomes also contained 2.5 mol% DHE and 1 mol% biotinylated PE, which allowed them to be anchored to streptavidin-coated coverslip dishes. TNBS quenching was measured by quantitative fluorescence microscopy. Images were first background corrected using a median filter, and then individual liposomes were identified using a combination of intensity (above an interactively chosen threshold) and size criteria. DHE fluorescence in individual liposomes was quantified before and after TNBS addition.

Approximately 50% of the DHE fluorescence was quenched by 10 mM TNBS, as expected for liposomes with 50% of the DHE in the outer leaflet (Figure 1). TNBS quenching of DHE was found to be insensitive to the composition of the liposomes because similar quenching behavior was observed in liposomes made either with lipids found in the outer leaflet or in the inner leaflet of the PM.

We also checked the quantum yield of DHE in these liposomes of varied compositions (Supplementary Figure S1). The DHE quantum yield in liposomes resembling outer leaflet was ~25% higher than for those resembling the inner

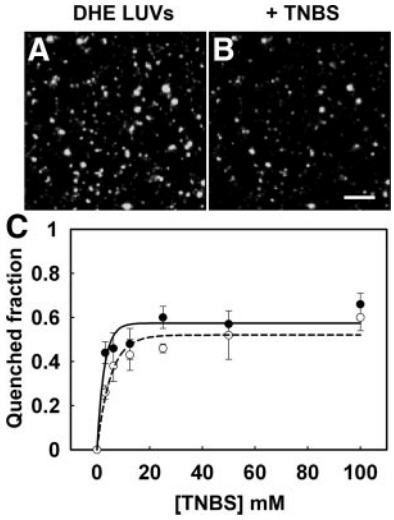

Figure 1. Quenching of DHE in liposomes by TNBS. TNBS quenches half the DHE fluorescence in unilamellar liposomes with a symmetrical interleaflet DHE distribution, and the quenching efficiency is similar in liposomes containing lipids resembling either outer leaflet lipids or inner leaflet lipids. Unilamellar vesicles were prepared by extrusion. Outer leaflet lipids were POPC:Egg:SM:cholesterol, 2.3:1.65:1, plus 2.5 mol% DHE and 1 mol% biotinylated PE. Inner leaflet lipids were POPC:POPE:POPS:cholesterol, 1.35:1.35:1.35:1, plus 2.5 mol% DHE and 1 mol% biotinylated PE. The liposomes were immobilized on streptavidin-coated coverslip dishes. (A and B) DHE fluorescence before and after addition of 10 mM TNBS to liposomes with outer leaflet lipid mixtures. (C) The concentration dependence of TNBS quenching of DHE fluorescence is shown by solid lines for outer leaflet lipid mixtures (●) and by dashed lines for inner leaflet lipid mixtures (○). Separate dishes were used for quenching with different concentrations of TNBS. Scale bar, 10 μm.

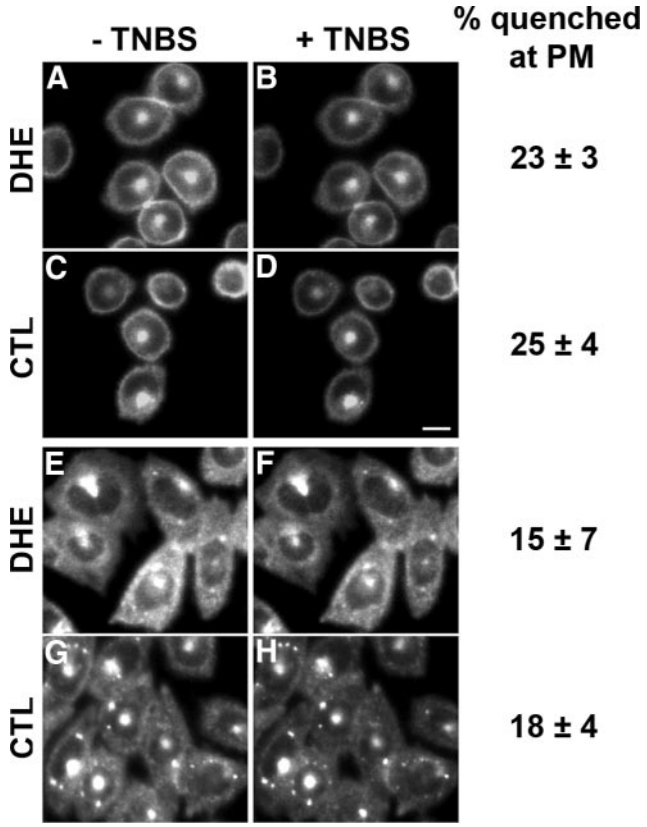

Figure 2. Quenching of DHE or CTL fluorescence by extracellular TNBS. TRVb1 cells were labeled with DHE-MβCD (A, B, E, and F) or CTL-MβCD (C, D, G, and H) for 1 min at 37°C, washed, and chased for 30 min. Before TNBS addition, DHE and CTL were distributed at the PM and the ERC (A, C, E, and G), with some additional punctate labeling for CTL (G). TNBS at 10 mM was added on the microscope stage, and images of the same fields were taken within 1 min (B, D, F, and H). All images were background corrected using off-cell fluorescence intensity. In displayed images, intensity was corrected for photobleaching by multiplying intensity values by an average correction factor that was determined in control photobleaching experiments. Scale bar, 10 μm. The quenching of fluorescence was measured in several regions at the circumference of 30–50 round cells per condition (A–D), and the quenching of fluorescence was measured in peripheral areas of more than 100 flat cells (E–H). Error estimates are SDs.

leaflet, and the fluorescence was only weakly dependent on cholesterol content. We did not correct for this difference in measurements in cells.

Extracellular TNBS Quenches a Small Fraction of PM-associated DHE or CTL Fluorescence

We then investigated the proportion of DHE or CTL in the outer leaflet of the PM by monitoring accessibility of these fluorescent sterols to the extracellular, membrane-impermeant quencher, TNBS. TRVb1 cells were labeled with DHE or CTL loaded onto MβCD for 1 min at 37°C, washed, and then incubated in medium 1 containing glucose for 30 min at 37°C in order to reach a steady-state distribution of DHE or CTL. Images of round cells focused near the cell center (Figure 2, A and C) showed DHE and CTL in a circumferential ring corresponding to the PM and a bright spot near the center of the cell, which is the ERC (Mukherjee *et al.*, 1998; Hao *et al.*, 2002). In flat, well-spread cells the ERC is the main site of intracellular DHE (Figure 2E) and CTL (Figure 2G), and the PM fluorescence in the periphery appears as a diffuse, hazy fluorescence. Some CTL was also observed in intracellular punctate structures (Figure 2G), which were identified as lipid droplets, based on Nile Red colabeling (not shown).

To measure quenching in the PM of living cells, we used two imaging protocols. For round cells, small regions at the outer perimeter were selected for measurement (examples shown in Supplementary Figure S2, A–C). Addition of 10 mM TNBS to cells labeled with either DHE or CTL quenched ~25% of the ring-like sterol fluorescence (Figure 2, B and D). For flat cells, we measured the fluorescence of several small regions in the periphery that showed uniform surrounding intensity (Supplementary Figure S2, D–F). This minimized contributions from intracellular organelles, and the cellular autofluorescence in these regions is <10% of the sterol fluorescence. When cells were treated with 10 mM TNBS, only 15–20% of the sterol fluorescence in these peripheral regions was quenched (Figure 2, F and H). No change in fluorescence above photobleaching was seen when medium 1 without TNBS was added (not shown).

Intracellular TNBS Efficiently Quenches DHE Fluorescence

The low quenching by TNBS suggests that most of the DHE and CTL is in the cytoplasmic leaflet of the PM and should be quenched by TNBS that has gained access to the cytoplasm. To open cells mechanically, nitrocellulose filters were placed over the cells and then removed to introduce holes in the membrane (Simons and Virta, 1987; Figure 3, A and B). Alternatively, cells were permeabilized by incubating with SLO (Martys *et al.*, 1995; Figure 3, C and D). Permeabilized cells (identified by nuclear staining with propidium iodide), exhibited DHE fluorescence in the remaining PM, and in the ERC (Figure 3, A and C). TNBS (10 mM) quenched most of the DHE fluorescence in the PM and the ERC in the permeabilized cells (Figure 3, B and D) but not in the neighboring unpermeabilized cells. Concentration-dependent quenching in permeabilized cells showed that 10 mM TNBS was sufficient to achieve maximal quenching, which was ~80% of the DHE fluorescence associated with the PM (Supplementary Figure S3).

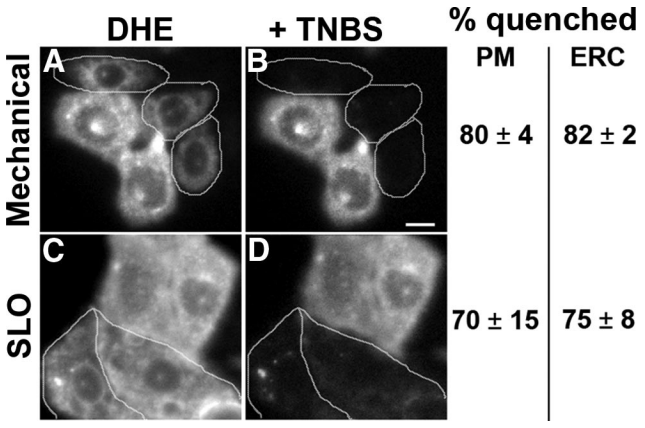

Figure 3. Quenching of PM- and ERC-associated DHE fluorescence by TNBS in permeabilized cells. TRVb1 cells were labeled with DHE-MβCD as for Figure 2. One set of cells was then permeabilized with nitrocellulose membrane overlay/removal (A and B). This opens the PM on the upper surface of some cells. Another set of cells was permeabilized with streptolysin-O (SLO; C and D). Images were acquired before (A and C) and after addition of 10 mM TNBS (B and D). Permeabilized cells, identified by propidium iodide staining, are outlined. Images have been background corrected using off-cell fluorescence intensity. Displayed images were corrected for photobleaching. Scale bar, 10 μm. The quenching of fluorescence in 30–50 cells for each condition was averaged. Error estimates are SDs.

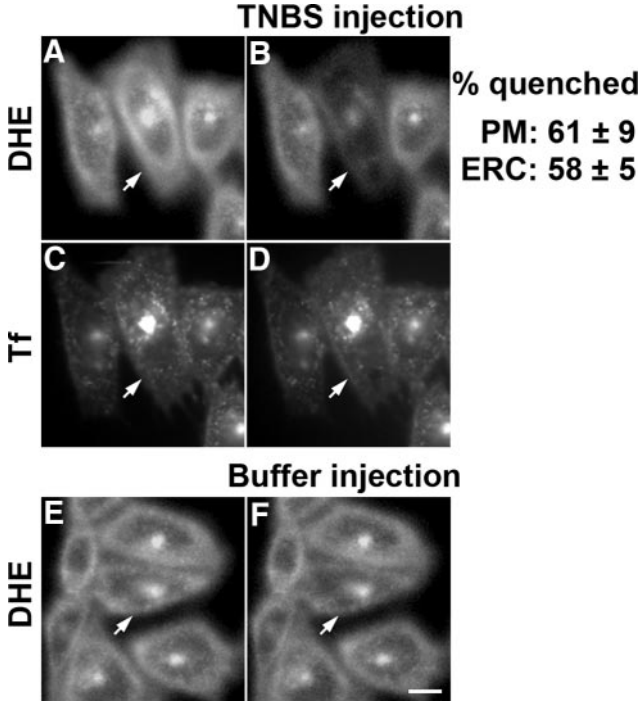

Figure 4. Quenching of fluorescence by microinjected TNBS. TRVb1 cells were labeled with DHE-MβCD for 1 min at 37°C, washed and chased for 30 min at 37°C, then further labeled with Tf-Alexa 633 (5 μg/ml) for 10 min at 37°C, washed, and imaged. A concentrated stock of 100 mM TNBS, along with Rh-dextran, was microinjected into the cells. Cell-associated fluorescence of DHE and Tf are shown before (A and C) and after (B and D) microinjection. A microinjection control is shown (E and F), in which buffer with Rh-dextran (without TNBS) was injected. Injected cells were identified by Rh-dextran and are shown by arrows. The fluorescence loss in buffer-injected cells was <5%. Images were background corrected using off-cell fluorescence intensity. Displayed images were corrected for photobleaching. Scale bar, 10 μm. The quenching of fluorescence in 15–20 cells for each condition was averaged. Error estimates are SDs.

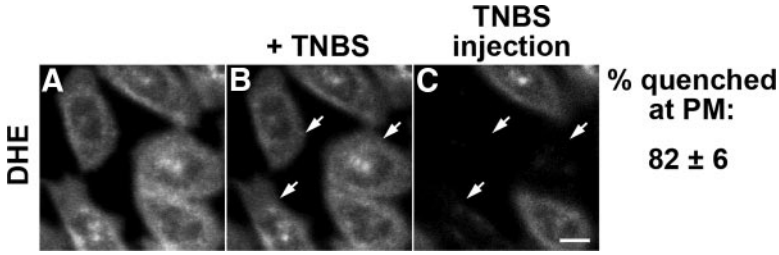

Figure 5. Extracellular TNBS delivery followed by TNBS microinjection quenches almost all the cell associated DHE fluorescence. TRVb1 cells were labeled with DHE-MβCD as described in the legend of Figure 2. DHE was distributed at the PM and the ERC (A). TNBS (10 mM) was added on the microscope stage, and an image of the same field was taken within 30 s (B). A concentrated stock of 100 mM TNBS, along with Rh-dextran was microinjected into a few cells of this same field and imaged immediately (C). Injected cells were identified by Rh-dextran labeling and shown by arrows. Images shown here have been background corrected using off-cell fluorescence intensity, and intensity was further corrected for photobleaching. Scale bar, 10 μm. The quenching of fluorescence in 29 cells in five microscopy fields was quantified and has been shown next to the images. Error values are SDs of quenching values.

We used microinjection to deliver TNBS (100 mM in the pipette) into the cytosol along with the fluorescent marker Rh-dextran. If the injection volume is ~5–10% of the cell volume (Lin *et al.*, 2002), the cytoplasmic TNBS concentration is expected to be ~5–10 mM. Injection of TNBS quenched the DHE fluorescence both at the cell periphery (mainly PM) and the ERC by ~60% (Figure 4, A and B). ERC integrity after TNBS injection was monitored by colabeling cells with Tf-Alexa 633. No change in Tf distribution or fluorescence intensity was observed in the ERC after injection (Figure 4, C and D). Injection of Rh-dextran without TNBS had no significant effect (<5% quenching) on the DHE fluorescence (Figure 4, E and F).

We next added TNBS (10 mM) extracellularly and then immediately microinjected the cells with TNBS to deliver the quencher to both leaflets. We found ~82% quenching of the cell-associated DHE fluorescence (Figure 5, A–C). The failure to obtain 100% quenching of DHE fluorescence in the cells is partially due to residual background and autofluorescence intensities, which account for ~5–10% of the fluorescence signal.

TNBS Quenching in Cells with High Levels of Fluorescent Sterol

Under our labeling conditions, DHE replaces ~5–10% of cell sterols (Wustner *et al.*, 2002). Thus, it is conceivable that the fluorescent sterol distribution we observed reflected the distribution preference for only a small fraction of the sterol in the cells. To obtain high levels of sterol replacement, we used the partial sterol auxotroph CHO cell line, M19 (Xu *et al.*, 2005). When M19 cells were grown for a week in the presence of DHE, about half of the cellular sterol was DHE. The DHE fluorescence was observed in the PM and the ERC, with occasional punctate structures that were identified as lipid droplets by colocalization with Nile Red (Figure 6 A and C; Nile Red colocalization not shown). The DHE fluorescence intensity of these cells was six times higher than cells labeled with a short pulse of DHE. Application of 8 mM TNBS did not greatly affect the DHE fluorescence in intact cells (Figure 6B), but SLO-permeabilized cells showed significant quenching of the DHE fluorescence (Figure 6D).

Other Outer Leaflet Lipid Quenchers Only Slightly Reduce DHE Fluorescence in the PM

To be certain that the results did not depend on the properties of the quencher, we tested several membrane-associated lipid quenchers. When incorporated into the outer leaflet of cells, 12-SLPC quenched the fluorescent lipid analog C_{12}-NBD-SM. NBD-labeled SM is incorporated into the outer leaflet of the PM, and flipping is slow because of the polar headgroup (Koval and Pagano, 1989; Mayor *et al.*, 1993). The 12-SLPC did not affect DHE fluorescence greatly (Supplementary Figure S4).

One concern with using long-chain lipid quenchers is that they need to be added to cells from stock solutions containing high concentrations of fatty acid–free BSA, which might extract certain lipids from the PM. To eliminate this problem, we used a more water-soluble spin-labeled lipid analog, 4-SLPC (Marx *et al.*, 1997). To validate the use of 4-SLPC as a quencher of DHE in the exofacial leaflet, we made vesicles (LUV) with lipid compositions that mimic those in the outer leaflet and the inner leaflet of the PM. Approximately 50% of the DHE fluorescence was quenched by 0.6 mM 4-SLPC, as expected for liposomes with 50% of the DHE in the outer leaflet (Supplementary Figure S5). When cells labeled with C_6-NBD-SM were exposed to 0.6 mM 4-SLPC, nearly all the PM-associated C_6-NBD-SM fluorescence was quenched (Figure 7, E and F). Addition of 4-SLPC to cells labeled with either DHE or CTL quenches only 10–20% of cell-associated sterol fluorescence (Figure 7, A–D). Ring-like CTL fluorescence in round cells is quenched by ~ 30% with 4-SLPC (Figure 7H).

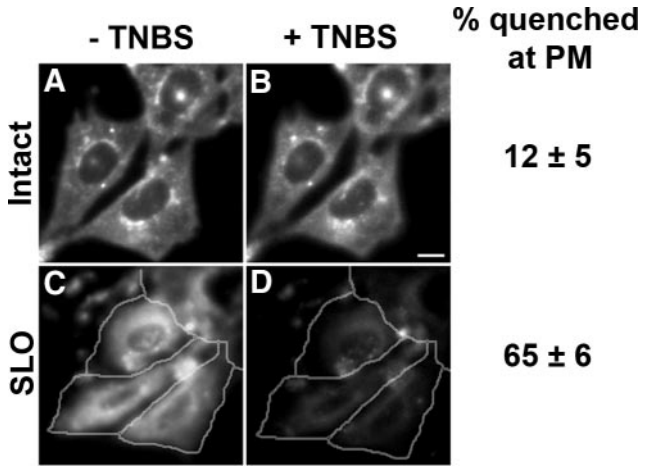

Figure 6. Quenching of DHE fluorescence in cells with 50% of sterol replaced by DHE. M19 cells were grown in DHE-LPDS for a week, and DHE fluorescence was imaged before (A) and after (B) addition of 8 mM TNBS. M19 cells growing in DHE-LPDS were permeabilized by SLO, and imaged before (C) and after (D) addition of 8 mM TNBS. Permeabilized cells, identified by propidium iodide staining, are outlined. Images have been background corrected using off-cell fluorescence intensity. The fluorescence intensity of these cells is about six times higher than that in cells labeled with short incubations. Displayed images were corrected for photobleaching. Scale bar, 10 μm. The quenching of fluorescence in 30–50 cells per condition was averaged. Error estimates are SDs.

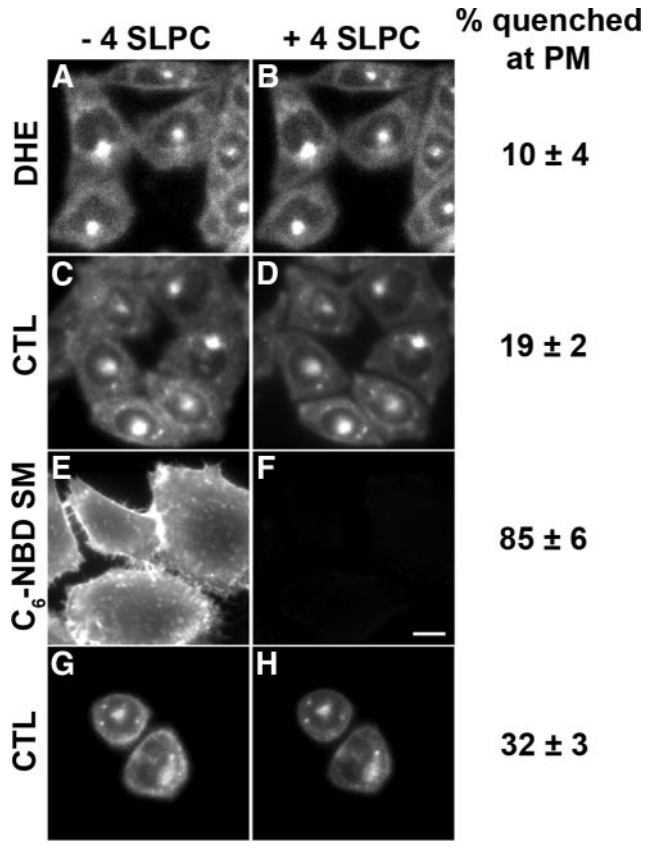

Figure 7. Quenching of C_6-NBD-SM, DHE, or CTL fluorescence by 4-SLPC. (A–D, G, and H) TRVb1 cells were labeled with DHE-MβCD or CTL- MβCD as for Figure 2. DHE and CTL images are shown before (A, C, and G) and after (B, D, and H) addition of 4-SLPC. (E and F) Plasma membranes of TRVb1 cells were labeled with C_6-NBD-SM and imaged before (E) or after (F) addition of 4-SLPC. Images were background corrected using off-cell fluorescence intensity. Displayed images were corrected for photobleaching. Scale bar, 10 μm. The quenching of peripheral fluorescence in ~100 cells was averaged for each condition. The quenching of circumferential fluorescence in ~30 round cells was averaged. Error estimates are SDs.

Microinjection of 4-SLPC into cells labeled with DHE quenched a significant amount of fluorescence both in the PM and in the ERC (Supplementary Figure S6, A and B). In contrast, the same injection of 4-SLPC in cells labeled with C_6-NBD-SM caused very little quenching in the ERC or in the PM (Supplementary Figure S6, E and F).

When 4-SLPC had access to both leaflets of the PM, first extracellularly and then by microinjection into the cytosol, we found a 76% loss of CTL fluorescence both from the PM and from the ERC of the injected cells (Figure 8).

DISCUSSION

Fluorescence of DHE or CTL in the PM is reduced only 15–30% by quenchers that have access solely to the outer leaflet of the bilayer. In contrast, the fluorescent sterols are quenched by ~60% in both the PM and the ERC when quenchers have access to the cytoplasmic leaflet and by 70–80% when both leaflets are accessible. These results show that the majority (≈60–70%) of sterol is in the cytoplasmic leaflet of the PM and the ERC. We note that the fraction of quenching in the circumferential fluorescence in round cells is somewhat higher than the fractional quenching observed in the periphery of flat cells. This may reflect the effect of fluorescent sterols in internal organelles in the periphery of the flat cells, which would not be quenched by external quenchers. Nevertheless, in the round cells, we only observe 23–32% quenching in the circumferential fluorescence. The DHE and CTL fluorescence in the ERC is very bright in relation to the surrounding areas, and we obtain ~65% quenching of this fluorescence upon microinjection of quenchers that would only have access to the cytoplasmic leaflet.

Relationship between Leaflet Lipid Composition and the Transbilayer Sterol Distribution

Lipid molecules most commonly found in the outer leaflet of the PM are phosphatidylcholine (PC) and sphingolipids, primarily SM. The sphingolipids in the PM are almost entirely in the outer leaflet (van Meer *et al.*, 2008). Several types of studies have been interpreted to indicate that there might be special interactions between sphingolipids and cholesterol, and this would presumably lead to a preponderance of sterol in the exofacial leaflet. For example, reduction in the amount of SM by sphingomyelinase treatment of cells leads to release of cholesterol from the PM, leading to increased esterification of cholesterol and a decrease in cholesterol biosynthesis (Slotte and Bierman, 1988; Gupta and Rudney, 1991).

Studies in model membranes have been interpreted to support the hypothesis that sphingomyelin and cholesterol interact preferentially in cells. Addition of cholesterol causes condensation of SM monolayers (Demel *et al.*, 1977). These and other observations led to the proposal that SM and cholesterol form "condensed complexes" (McConnell and Vrljic, 2003). However, such an interaction is not unique to sphingolipids. Similar cholesterol-dependent condensations have been reported for PC, and the condensation was found to be dependent on the hydrocarbon chain chemistry of PC (Smaby *et al.*, 1994). Specifically, one of the acyl chains (the *sn*-1 chain) of the PC had to be long and capable of adopting an extended configuration (i.e., no *cis* unsaturation). In a more general model, it has been suggested that cholesterol interacts favorably with any lipids that have relatively saturated tails and large head groups (Ali *et al.*, 2007).

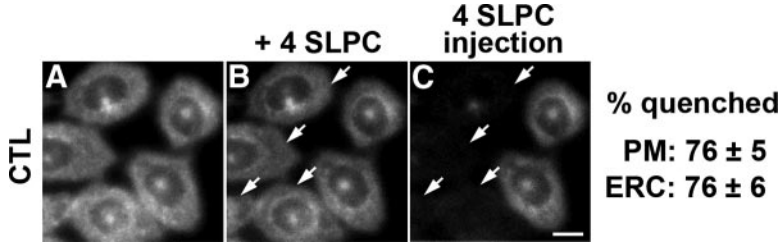

Figure 8. Extracellular 4-SLPC delivery followed by 4-SLPC microinjection quenches most of the PM- and ERC-associated CTL fluorescence. TRVb1 cells were labeled with CTL-MβCD as for Figure 2 A. 4-SLPC (0.6 mM) was added on the microscope stage and an image of the same field was taken within 30 s (B). A concentrated stock of 25 mM 4-SLPC was microinjected into a few cells (arrows) of this same field and imaged immediately (C). Images were background corrected using off-cell fluorescence intensity. Displayed images were corrected for photobleaching. Scale bar, 10 μm. The quenching of fluorescence in 30 injected cells was averaged. Error estimates are SDs.

The inner leaflet of the PM contains mainly glycerophospholipids, predominantly PE, PS, and PC (Op den Kamp, 1979; Pomorski and Menon, 2006). Interestingly, the acyl chains of several of these lipid classes (most notably PC and PS) contain more saturated fatty acyl chains in the PM than in other cellular membranes (Fridriksson *et al.*, 1999). These saturated acyl chain inner leaflet lipids should be able to accommodate cholesterol approximately as well as SM does.

Treatment of cells with sphingomyelinase, which creates ceramide, may have complex effects. Ceramide has a relatively high flip-flop rate in membranes (Bai and Pagano, 1997; Lopez-Montero *et al.*, 2005). Like cholesterol, ceramide has a relatively small polar head group, and it has been shown to compete with cholesterol for sites in ordered domains of membranes (Megha and London, 2004). Thus, sphingomyelinase treatment of cells could displace cholesterol from the cytoplasmic leaflet of the PM by increasing the ceramide content in the cytoplasmic leaflet.

In a living cell, lipid flipping or other active processes such as lipid metabolism and membrane deformations (e.g., budding or tubulation) could reduce the relative proportion of lipids in the cytoplasmic leaflet, and sterols could flip as required to fill the gaps. Further studies will be required to understand the mechanistic basis for the asymmetric transbilayer distribution of cholesterol in the PM and the ERC membrane.

Implications of the Localization of Large Amounts of Sterol in the Inner Leaflet of the PM and the Outer Leaflet of the ERC

We find that roughly 60–70% of the PM and ERC sterol resides in the inner leaflet. If cholesterol is 30 mol% of PM lipids (Lange *et al.*, 1989; Warnock *et al.*, 1993), and 65% of it resides in the inner leaflet, ~40 mol% of lipids in the inner leaflet are sterol. The solubility limit for cholesterol has been measured to be 66 mol% in PC and 51 mol% in PE bilayers (Huang *et al.*, 1999).

Such a transbilayer distribution of cholesterol may have important implications for cholesterol transport. A large fraction of intracellular cholesterol transport is carried out by nonvesicular mechanisms (Hao *et al.*, 2002), and cholesterol on the cytoplasmic leaflet would be readily available for transfer to a cytoplasmic carrier. These transport processes can be quite rapid. For example, the sterol in the ERC reequilibrates with other sterol pools (mainly PM) in the cell with a $t_{1/2}$ of ~2.5 min (Hao *et al.*, 2002). This rapid nonvesicular transport could allow organelles such as the endoplasmic reticulum to respond very quickly to changes in sterol levels in the PM (Maxfield and Wustner, 2002; Lange *et al.*, 2008). In contrast to the very rapid intracellular transport of cholesterol, export of cholesterol to extracellular acceptors such as high-density lipoprotein or apolipoprotein A-I is relatively slow, with a few percent of cellular cholesterol released per hour (Rothblat *et al.*, 1992). The low abundance of cholesterol in the outer leaflet might contribute to the slow release of cholesterol to protein acceptors.

A large proportion of PM and ERC sterol localized in the cytoplasmic leaflet could provide a mechanism to organize cytoplasmic leaflet liquid ordered domains, which have been reported to exist concomitant with ordered domains on the outer leaflet (Pyenta *et al.*, 2001; Devaux and Morris, 2004). It would be worthwhile to reconsider some physical properties of the PM and ERC in the light of our current findings.

ACKNOWLEDGMENTS

We thank Dr. T. Y. Chang (Dartmouth College, Hanover, NH) for providing the M19 cell line, Dr. G. W. Feigenson (Cornell University, Ithaca, NY) for providing the initial batch of CTL, Dr. J. D. Warren (Weill Cornell Medical College, NY) for chemical synthesis of CTL and 4-SLPC, Dr. R. Deckelbaum and I. Hanson (College of Physicians and Surgeons, Columbia University, New York, NY) for assistance with gas chromatography, and Harold Ralph for writing a journal for analysis of liposome data. This work was supported by National Institutes of Health Grant DK27083 and by a grant from the Ara Parseghian Medical Research Foundation.

REFERENCES

Ali, M. R., Cheng, K. H., and Huang, J. (2007). Assess the nature of cholesterol-lipid interactions through the chemical potential of cholesterol in phosphatidylcholine bilayers. Proc. Natl. Acad. Sci. USA *104*, 5372–5377.

Bai, J., and Pagano, R. E. (1997). Measurement of spontaneous transfer and transbilayer movement of BODIPY-labeled lipids in lipid vesicles. Biochemistry *36*, 8840–8848.

Bjorkqvist, Y. J., Nyholm, T. K., Slotte, J. P., and Ramstedt, B. (2005). Domain formation and stability in complex lipid bilayers as reported by cholestatrienol. Biophys. J. *88*, 4054–4063.

Blau, L., and Bittman, R. (1978). Cholesterol distribution between the two halves of the lipid bilayer of human erythrocyte ghost membranes. J. Biol. Chem. *253*, 8366–8368.

Boesze-Battaglia, K., Clayton, S. T., and Schimmel, R. J. (1996). Cholesterol redistribution within human platelet plasma membrane: evidence for a stimulus-dependent event. Biochemistry *35*, 6664–6673.

Brasaemle, D. L., Robertson, A. D., and Attie, A. D. (1988). Transbilayer movement of cholesterol in the human erythrocyte membrane. J. Lipid Res. *29*, 481–489.

Demel, R. A., Jansen, J. W., van Dijck, P. W., and van Deenen, L. L. (1977). The preferential interaction of cholesterol with different classes of phospholipids. Biochim. Biophys. Acta *465*, 1–10.

Devaux, P. F., and Morris, R. (2004). Transmembrane asymmetry and lateral domains in biological membranes. Traffic *5*, 241–246.

Dietrich, C., Bagatolli, L. A., Volovyk, Z. N., Thompson, N. L., Levi, M., Jacobson, K., and Gratton, E. (2001). Lipid rafts reconstituted in model membranes. Biophys. J. *80*, 1417–1428.

Fellmann, P., Zachowski, A., and Devaux, P. F. (1994). Synthesis and use of spin-labeled lipids for studies of the transmembrane movement of phospholipids. Methods Mol. Biol. *27*, 161–175.

Fischer, R. T., Stephenson, F. A., Shafiee, A., and Schroeder, F. (1984). delta 5,7,9(11)-Cholestatrien-3 beta-ol: a fluorescent cholesterol analogue. Chem. Phys. Lipids *36*, 1–14.

Fisher, K. A. (1976). Analysis of membrane halves: cholesterol. Proc. Natl. Acad. Sci. USA *73*, 173–177.

Fridriksson, E. K., Shipkova, P. A., Sheets, E. D., Holowka, D., Baird, B., and McLafferty, F. W. (1999). Quantitative analysis of phospholipids in functionally important membrane domains from RBL-2H3 mast cells using tandem high-resolution mass spectrometry. Biochemistry *38*, 8056–8063.

Gottlieb, M. H. (1977). The reactivity of human erythrocyte membrane cholesterol with a cholesterol oxidase. Biochim. Biophys. Acta *466*, 422–428.

Gupta, A. K., and Rudney, H. (1991). Plasma membrane sphingomyelin and the regulation of HMG-CoA reductase activity and cholesterol biosynthesis in cell cultures. J. Lipid Res. *32*, 125–136.

Hale, J. E., and Schroeder, F. (1982). Asymmetric transbilayer distribution of sterol across plasma membranes determined by fluorescence quenching of dehydroergosterol. Eur. J. Biochem. *122*, 649–661.

Hao, M., Lin, S. X., Karylowski, O. J., Wustner, D., McGraw, T. E., and Maxfield, F. R. (2002). Vesicular and non-vesicular sterol transport in living cells. The endocytic recycling compartment is a major sterol storage organelle. J. Biol. Chem. *277*, 609–617.

Hao, M., Mukherjee, S., and Maxfield, F. R. (2001). Cholesterol depletion induces large scale domain segregation in living cell membranes. Proc. Natl. Acad Sci. USA *98*, 13072–13077.

Hayashi, H., Igbavboa, U., Hamanaka, H., Kobayashi, M., Fujita, S. C., Wood, W. G., and Yanagisawa, K. (2002). Cholesterol is increased in the exofacial leaflet of synaptic plasma membranes of human apolipoprotein E4 knock-in mice. Neuroreport *13*, 383–386.

Huang, J., Buboltz, J. T., and Feigenson, G. W. (1999). Maximum solubility of cholesterol in phosphatidylcholine and phosphatidylethanolamine bilayers. Biochim. Biophys. Acta *1417*, 89–100.

Hyslop, P. A., Morel, B., and Sauerheber, R. D. (1990). Organization and interaction of cholesterol and phosphatidylcholine in model bilayer membranes. Biochemistry *29*, 1025–1038.

Koval, M., and Pagano, R. E. (1989). Lipid recycling between the plasma membrane and intracellular compartments: transport and metabolism of fluorescent sphingomyelin analogues in cultured fibroblasts. J. Cell Biol. *108*, 2169–2181.

Lange, Y., Ory, D. S., Ye, J., Lanier, M. H., Hsu, F. F., and Steck, T. L. (2008). Effectors of rapid homeostatic responses of endoplasmic reticulum cholesterol and 3-hydroxy-3-methylglutaryl-CoA reductase. J. Biol. Chem. *283*, 1445–1455.

Lange, Y., Swaisgood, M. H., Ramos, B. V., and Steck, T. L. (1989). Plasma membranes contain half the phospholipid and 90% of the cholesterol and sphingomyelin in cultured human fibroblasts. J. Biol. Chem. *264*, 3786–3793.

Lin, S. X., Gundersen, G. G., and Maxfield, F. R. (2002). Export from pericentriolar endocytic recycling compartment to cell surface depends on stable, detyrosinated (glu) microtubules and kinesin. Mol. Biol. Cell *13*, 96–109.

Lopez-Montero, I., Rodriguez, N., Cribier, S., Pohl, A., Velez, M., and Devaux, P. F. (2005). Rapid transbilayer movement of ceramides in phospholipid vesicles and in human erythrocytes. J. Biol. Chem. *280*, 25811–25819.

Martys, J. L., Shevell, T., and McGraw, T. E. (1995). Studies of transferrin recycling reconstituted in streptolysin O permeabilized Chinese hamster ovary cells. J. Biol. Chem. *270*, 25976–25984.

Marx, U., Lassmann, G., Wimalasena, K., Muller, P., and Herrmann, A. (1997). Rapid kinetics of insertion and accessibility of spin-labeled phospholipid analogs in lipid membranes: a stopped-flow electron paramagnetic resonance approach. Biophys. J. *73*, 1645–1654.

Maxfield, F. R., and Wustner, D. (2002). Intracellular cholesterol transport. J. Clin. Invest. *110*, 891–898.

Mayer, L. D., Hope, M. J., and Cullis, P. R. (1986). Vesicles of variable sizes produced by a rapid extrusion procedure. Biochim. Biophys. Acta *858*, 161–168.

Mayor, S., Presley, J. F., and Maxfield, F. R. (1993). Sorting of membrane components from endosomes and subsequent recycling to the cell surface occurs by a bulk flow process. J. Cell Biol. *121*, 1257–1269.

McConnell, H. M., and Vrljic, M. (2003). Liquid-liquid immiscibility in membranes. Annu. Rev. Biophys. Biomol. Struct. *32*, 469–492.

McGraw, T. E., Greenfield, L., and Maxfield, F. R. (1987). Functional expression of the human transferrin receptor cDNA in Chinese hamster ovary cells deficient in endogenous transferrin receptor. J. Cell Biol. *105*, 207–214.

Megha, and London, E. (2004). Ceramide selectively displaces cholesterol from ordered lipid domains (rafts): implications for lipid raft structure and function. J. Biol. Chem. *279*, 9997–10004.

Mukherjee, S., Soe, T. T., and Maxfield, F. R. (1999). Endocytic sorting of lipid analogues differing solely in the chemistry of their hydrophobic tails. J. Cell Biol. *144*, 1271–1284.

Mukherjee, S., Zha, X., Tabas, I., and Maxfield, F. R. (1998). Cholesterol distribution in living cells: fluorescence imaging using dehydroergosterol as a fluorescent cholesterol analog. Biophys. J. *75*, 1915–1925.

Op den Kamp, J. A. (1979). Lipid asymmetry in membranes. Annu. Rev. Biochem. *48*, 47–71.

Pomorski, T., and Menon, A. K. (2006). Lipid flippases and their biological functions. Cell Mol. Life Sci. *63*, 2908–2921.

Pyenta, P. S., Holowka, D., and Baird, B. (2001). Cross-correlation analysis of inner-leaflet-anchored green fluorescent protein co-redistributed with IgE receptors and outer leaflet lipid raft components. Biophys. J. *80*, 2120–2132.

Rothblat, G. H., Mahlberg, F. H., Johnson, W. J., and Phillips, M. C. (1992). Apolipoproteins, membrane cholesterol domains, and the regulation of cholesterol efflux. J. Lipid Res. *33*, 1091–1097.

Salzman, N. H., and Maxfield, F. R. (1989). Fusion accessibility of endocytic compartments along the recycling and lysosomal endocytic pathways in intact cells. J. Cell Biol. *109*, 2097–2104.

Scheidt, H. A., Muller, P., Herrmann, A., and Huster, D. (2003). The potential of fluorescent and spin-labeled steroid analogs to mimic natural cholesterol. J. Biol. Chem. *278*, 45563–45569.

Schroeder, F., Nemecz, G., Wood, W. G., Joiner, C., Morrot, G., Ayraut-Jarrier, M., and Devaux, P. F. (1991). Transmembrane distribution of sterol in the human erythrocyte. Biochim. Biophys. Acta *1066*, 183–192.

Schroeder, R. J., Ahmed, S. N., Zhu, Y., London, E., and Brown, D. A. (1998). Cholesterol and sphingolipid enhance the Triton X-100 insolubility of glycosylphosphatidylinositol-anchored proteins by promoting the formation of detergent-insoluble ordered membrane domains. J. Biol. Chem. *273*, 1150–1157.

Simons, K., and Virta, H. (1987). Perforated MDCK cells support intracellular transport. EMBO J. *6*, 2241–2247.

Slotte, J. P., and Bierman, E. L. (1988). Depletion of plasma-membrane sphingomyelin rapidly alters the distribution of cholesterol between plasma membranes and intracellular cholesterol pools in cultured fibroblasts. Biochem. J. *250*, 653–658.

Smaby, J. M., Brockman, H. L., and Brown, R. E. (1994). Cholesterol's interfacial interactions with sphingomyelins and phosphatidylcholines: hydrocarbon chain structure determines the magnitude of condensation.[erratum appears in Biochemistry 1997 Feb 25;36(8):2338]. Biochemistry *33*, 9135–9142.

Steck, T. L., Ye, J., and Lange, Y. (2002). Probing red cell membrane cholesterol movement with cyclodextrin. Biophys. J. *83*, 2118–2125.

van Meer, G., Voelker, D. R., and Feigenson, G. W. (2008). Membrane lipids: where they are and how they behave. Nat. Rev. Mol. Cell Biol. *9*, 112–124.

Wang, J., Megha, and London, E. (2004). Relationship between sterol/steroid structure and participation in ordered lipid domains (lipid rafts): implications for lipid raft structure and function. Biochemistry *43*, 1010–1018.

Wang, T. Y., and Silvius, J. R. (2001). Cholesterol does not induce segregation of liquid-ordered domains in bilayers modeling the inner leaflet of the plasma membrane. Biophys. J. *81*, 2762–2773.

Warnock, D. E., Roberts, C., Lutz, M. S., Blackburn, W. A., Young, W. W., Jr., and Baenziger, J. U. (1993). Determination of plasma membrane lipid mass and composition in cultured Chinese hamster ovary cells using high gradient magnetic affinity chromatography. J. Biol. Chem. *268*, 10145–10153.

Wustner, D. (2007). Plasma membrane sterol distribution resembles the surface topography of living cells. Mol. Biol. Cell *18*, 211–228.

Wustner, D., Herrmann, A., Hao, M., and Maxfield, F. R. (2002). Rapid nonvesicular transport of sterol between the plasma membrane domains of polarized hepatic cells. J. Biol. Chem. *277*, 30325–30336.

Xu, F., Rychnovsky, S. D., Belani, J. D., Hobbs, H. H., Cohen, J. C., and Rawson, R. B. (2005). Dual roles for cholesterol in mammalian cells. Proc. Natl. Acad Sci. USA *102*, 14551–14556.

Yeung, T., Gilbert, G. E., Shi, J., Silvius, J., Kapus, A., and Grinstein, S. (2008). Membrane phosphatidylserine regulates surface charge and protein localization. Science *319*, 210–213.